Laser speckle contrast imaging is sensitive to advective flux

Kosar Khaksari
Sean J. Kirkpatrick

Laser speckle contrast imaging is sensitive to advective flux

Kosar Khaksari[,†] and Sean J. Kirkpatrick[*]
Michigan Technological University, Department of Biomedical Engineering, 1400 Townsend Drive, Houghton, Michigan 49931, United States

Abstract. Unlike laser Doppler flowmetry, there has yet to be presented a clear description of the physical variables that laser speckle contrast imaging (LSCI) is sensitive to. Herein, we present a theoretical basis for demonstrating that LSCI is sensitive to total flux and, in particular, the summation of diffusive flux and advective flux. We view LSCI from the perspective of mass transport and briefly derive the diffusion with drift equation in terms of an LSCI experiment. This equation reveals the relative sensitivity of LSCI to both diffusive flux and advective flux and, thereby, to both concentration and the ordered velocity of the scattering particles. We demonstrate this dependence through a short series of flow experiments that yield relationships between the calculated speckle contrast and the concentration of the scatterers (manifesting as changes in scattering coefficient), between speckle contrast and the velocity of the scattering fluid, and ultimately between speckle contrast and advective flux. Finally, we argue that the diffusion with drift equation can be used to support both Lorentzian and Gaussian correlation models that relate observed contrast to the movement of the scattering particles and that a weighted linear combination of these two models is likely the most appropriate model for relating speckle contrast to particle motion. © *The Authors. Published by SPIE under a Creative Commons Attribution 3.0 Unported License. Distribution or reproduction of this work in whole or in part requires full attribution of the original publication, including its DOI.* [DOI: 10.1117/1.JBO.21.7.076001]

1 Introduction

Laser speckle contrast imaging (LSCI) is a noninvasive (or minimally invasive) imaging modality used primarily for the relative and qualitative imaging of blood flow and perfusion.[1–3] This method has a wide field of view, and it is efficient and simple for full-field monitoring. The simplicity of LSCI along with its high spatial and temporal resolution allows it to be used as a powerful tool to measure, monitor, and investigate living processes in near real-time. The fundamental concept behind this method is the quantification of the relationship between moving particles (scatterers) in the object space (i.e., the living organ or blood vessel) and the moving speckles in the image plane. When there is motion in the object space, the intensity of speckles in the image space fluctuates in time. It is these time-varying speckles in the image space that encode the motion in the scattering object. In time-varying, or dynamic, speckle patterns, the speckle is blurred during the finite camera integration time and the spatial variation, or contrast, in intensity is thereby decreased.

A clear relationship between LSCI and laser Doppler flowmetry (LDF) has been established in the literature.[2] Furthermore, a clear relationship between LDF and both the concentration of scattering particles and the velocity of the particle-containing fluid has been established.[4] As noted by Boas and Dunn,[2] the theoretical basis of LSCI seems to imply that LSCI is sensitive to variations in speed, yet several authors have observed that LSCI is sensitive to particle concentration as well.[2,5] This implies that LSCI is truly a measure of flux.

However, a clear demonstration of this has yet to be presented, which is the purpose of this paper.

1.1 Blood Perfusion, Flow, Speed, Velocity, and Flux

In order to more clearly understand exactly what LSCI is sensitive to, it is important to have clear definitions of the various terms used in the literature to describe the movement of blood. Many of these terms have been used interchangeably in the LSCI literature, even though these terms possess different units and physical dimensions.[2,3]

Clinical units for blood perfusion are typically milliliters (of blood) per milliliters (of tissue) per second (ml/ml/s) and is a measure of blood volume flow through a given volume or mass of tissue. Blood perfusion clearly indicates a rate, $\phi_b = (V_b/V_t)/s$, where V_b is the volume of whole blood, V_t is the volume of tissue, and s is seconds. Alternatively, blood perfusion may be reported in units of ml/100 mg/min. Either way, clinical blood perfusion is a measure of capillary and interstitial blood flow and is meant as a means of quantifying the delivery of oxygen and nutrients to the tissue as well as the removal rate of metabolic waste from the tissue by the blood. Regardless of units, blood perfusion has physical dimensions of [quantity] T^{-1} (because $M \propto L^3$). It should be noted that V_b refers to the volume of whole blood, not just the components of blood that scatter light. The units of blood perfusion imply a concentration rate.

The term flow is usually expressed in terms of volume per time, e.g., ml/s, and has physical dimensions of L^3/T. The frequency shift observed in LDF of blood has been convincingly demonstrated to be sensitive to bulk blood flow and to particle density.[4] Flow, when discussing the movement of a fluid with

---

†Present address: University of Washington, Department of Bioengineering, 3720 15th Avenue NorthEast, Seattle, Washington 98105, United States.

suspended particles, such as blood, is often thought of as the number of particles per volume per time,[2] or a concentration rate, $[\dot{c}]$, where the dot explicitly indicates the time derivative and $[c]$ is the number concentration, $[c] = (n_p/V_b)$, where n_p is the number of particles. In this case, flow is more properly referred to as flux density (below).

Speed and velocity are often used interchangeably, although they are two very different quantities.[3] Speed is a scalar quantity with units of distance per time (e.g., ms^{-1}, while velocity is a vector quantity with the same units. The magnitude of the velocity vector is speed. Both speed and velocity have physical dimensions of LT^{-1}.

Flux is a term used to describe transport phenomena, i.e., the flow of some physical property (mass, energy, momentum, and so on) in space. It is typically thought of as a rate of flow of a physical property per unit area. Flux has the physical dimensions of [quantity] $T^{-1}L^{-2}$. Of particular relevance to LSCI is the diffusive flux [the rate of movement of particles across a unit area (e.g., $mol\,m^{-2} \cdot s^{-1}$)], which describes Fick's first law of diffusion and advective flux ([particles] $m^{-2}\,s^{-1}$), where the square brackets indicate the number concentration.[6]

1.2 Relationship to Laser Doppler Flowmetry

In addressing the issue of what LSCI is sensitive to, the usual approach is to observe that LSCI and LDF essentially measure the same quantity, although through very different means.[3] Goodman[7] established a relationship between the speckle contrast, $K = \sigma_s/\langle I \rangle$, and the autocovariance of the intensity fluctuations, $C_t(\tau)$, of an individual speckle[3]

$$K^2 \propto \sigma_s^2(T) = \frac{1}{T}\int_0^T C_t(\tau)d\tau, \tag{1}$$

where T is the detector integration time, τ is the characteristic correlation time, and σ^2 is the speckle intensity variance over time T. The autocovariance of the intensity fluctuations, $C_t(\tau)$, was assumed to follow a Lorentzian distribution, although this assumption is not a necessity for Eq. (1) to hold. By assuming a Lorentzian line shape for $C_t(\tau)$, it is implicit that the underlying particle motions giving rise to the intensity fluctuations is random (Brownian for larger particles). If ordered motion is assumed, then $C_t(\tau)$ follows a Gaussian line shape.[8] LDF directly evaluates the integrand on the right-hand side (RHS) of Eq. (1), while LSCI indirectly assesses the left-hand side of the equation. [3]

Bonner and Nossal[4] clearly demonstrated a quantitative relationship between the mean Doppler shift, $\langle \omega \rangle$, particle density, and velocity of the fluid in a moving fluid, i.e., a dependence of $\langle \omega \rangle$ on particle flux. Yet, such a clear demonstration has not yet been provided for LSCI. The remainder of this paper considers LSCI from the perspective of mass transport and aims to demonstrate a theoretical and experimental dependence of LSCI on particle flux.

2 Theory

2.1 Diffusion with Drift Equations

We begin by viewing the problem in terms of a three-dimensional (3-D) mass-transport problem governed by the convection-diffusion equations. [6] In the most general 3-D form, the convection-diffusion equation is frequently given as

$$\frac{\partial[c]}{\partial t} = R + \nabla \cdot [D\nabla(c)] - \nabla \cdot [\vec{v}(c)], \tag{2}$$

where $[c]$ is the concentration of scatterers (e.g., red blood cells), D is the mass diffusivity for the scattering particle motion and is simply diffusion coefficient of the scatterers, R is a factor that accounts for a change in the number of scatterers due to creation or destruction (also referred to as a "source" or "sink" of $[c]$), and $\vec{v}$ is the average velocity of the moving scatterers, which in our case we will assume is the average blood flow velocity $(m\,s^{-1})$. As usual, $\nabla \cdot$ represents the divergence and ∇ is the gradient in the dimensions $[x, y, $ and $z]$.

Several simplifying assumptions can be made for our situation.[6] We assume a steady-state situation such that $(\partial[c]/\partial t) = 0$, over the camera integration time, i.e., the concentration of scatterers remains constant over the imaging time. Second, we assume that the overall number of scatterers remains constant in our imaging volume over the imaging time, i.e., $R = 0$. Given these assumptions, then, Eq. (2) becomes the stationary convection-diffusion equation

$$0 = \nabla \cdot (D\nabla[c]) - \nabla \cdot (\vec{v}[c]). \tag{3}$$

The first term on the RHS of the equation, $\nabla \cdot (D\nabla[c])$, describes the flux J_L due to random motion of the scatterers and in mass-transport theory is usually attributed to diffusion. The local motion of the scatterers is random and in spectroscopic or laser physics terminology is described by a Lorentzian spectral line shape.[8] Employing an analogy from laser physics, all of the scatterers in the imaging volume will have identical behaviors. In laser physics, this results in the phenomenon of homogeneous line broadening and is one of the two possible limiting behaviors of moving particles. The second term on the RHS of the equation $\nabla \cdot (\vec{v}[c])$ describes the flux J_G due to both the concentration of the scatterers and the velocity of the fluid (blood serum). This term is referred to as advective flux. Advection is defined here as the transport mechanism by which the scatterers (e.g., red blood cells) are transported due to the bulk motion of the fluid, the blood serum. The advection operator in Cartesian coordinates can be given as[6]

$$\nabla \cdot \mathbf{v} = \vec{v}_x\frac{\partial}{\partial x} + \vec{v}_y\frac{\partial}{\partial y} + \vec{v}_z\frac{\partial}{\partial z}, \tag{4}$$

where $\mathbf{v}$ is a velocity field. If the flow is assumed to be incompressible then $\mathbf{v}$ is solenoidal (i.e., $\nabla \cdot \mathbf{v} = 0$) and the advection equation may be written as

$$\frac{\partial\varphi}{\partial t} + \mathbf{v} \cdot \nabla\varphi = 0, \tag{5}$$

where φ is a scalar field that describes the location of the scattering particles. If the flow of the blood serum is steady then $\mathbf{v} \cdot \nabla\varphi = 0$, φ is steady along a streamline and the flow is organized. As above, in the terminology of laser physics, this can be viewed as an inhomogeneous line broadening phenomenon and the dynamic behavior is particular to individual scatterers. The line shape for the population of scatterers in this case is Gaussian[8] and represents the other possible limiting behavior (as opposed to the Lorentzian description, above).

Thus, Eq. (3) describes ordered and unordered flow, along with both the diffusion-dependent and velocity-dependent components of the total flux $J_{KK} = J_L + J_G$. In the case where the

motion is entirely due to random motion (Brownian), then $J_G = 0$. In the other limiting case where the motion is purely organized flow, $J_L = 0$. Of course, these two limiting situations are rare, and in most cases of practical interests, there will be components of both types of motion.

For the sake of thoroughness, it is worth noting that the average velocity $\vec{v}$ is in some fashion proportional to the applied pressure (i.e., the blood pressure). In this case, we can write the stationary drift-diffusion equation [6]

$$0 = \nabla \cdot (D\nabla[c]) - \nabla \cdot \left(\frac{\vec{F}c}{\xi}\right), \tag{6}$$

where $\vec{F}$ is the applied force and ξ describes the viscous drag on the particles (e.g., the red blood cells).

In the case of perfusion imaging using LSCI, the dimensionality of the problem can be reduced to two dimensions, x and y (assuming the optical imaging axis is in the z-direction). The situation becomes planar when one realizes that LSCI is a coherent imaging technique and that the light scattered from all scatterers within the depth of field (DOF) of the imaging lens will coherently sum in the imaging plane to create a single speckle pattern. The underlying assumption is that the temporal coherence length of the laser, $\ell_c \geq$ DOF. In the planar assumption, the convection-diffusion equation [Eq. (3)] is recognized as Fick's first equation with drift[9]

$$J_x = -D\frac{\partial[c]}{\partial x} + \vec{v}_x[c], \quad J_y = -D\frac{\partial[c]}{\partial y} + \vec{v}_y[c], \tag{7}$$

which describes the situation in which all of the scatterers translate in the $+x$ (or $+y$) direction at a velocity $\vec{v}$. Thus, the flux at any point x increases by amount $\vec{v}_x[c](x)$ (and similarly for any point y).

Equation (7) may also be written in a form that incorporates the applied force $\vec{F}$, such as blood pressure, that is responsible for the "drift" [i.e., the second term on the RHS of Eq. (7)]. In this case, Eq. (7) becomes

$$J_x = -D\frac{\partial[c]}{\partial x} + \frac{\vec{F}_x}{\xi}[c], \quad J_y = -D\frac{\partial[c]}{\partial y} + \frac{\vec{F}_y}{\xi}[c]. \tag{8}$$

In many LSCI applications where the motion along a vessel is of interest, Eq. (7) can be further reduced in dimensionality to a one-dimensional (1-D) problem. As with the discussion of Eq. (3), Eq. (7) describes ordered and unordered flow, along with both the diffusion-dependent (first term on the RHS) and velocity-dependent (second term on the RHS) components of the total flux.

We now focus on a situation in which the movement of scattering particles is entirely random (Brownian motion). Such a situation may be envisioned when using LSCI to image a semi-infinite medium with scattering particles (e.g., microspheres) in random motion. Thus,

$$J_{KK} \propto \frac{\partial[c]}{\partial x}. \tag{9}$$

Therefore, in this implementation, LSCI is sensitive to diffusional flux resulting from a concentration gradient or from the Brownian motion of particles.

In the case of primarily ordered flow (i.e., steady flow in a vessel or tube), it is seen that

$$J_{KK} \cong \vec{v}[c], \tag{10}$$

which describes the condition in which the total flux is due entirely to advective flux. Advective flux is a flux that is dependent upon both velocity $\vec{v}$ and concentration of scattering particles $[c]$.[6] Thus in this implementation, LSCI is sensitive to flux resulting from both velocity and concentration of scatterers. An increase in either velocity or concentration will result in an increase in the number of dynamic scattering events during a given time interval (camera integration time, T), resulting in a decrease in contrast, K.

To relate this discussion to our assertion at the top of this section that our problem is one of mass transport, we note that advective flux as defined by Eq. (10) is related to the total mass flux $\dot{m}$ across a plane perpendicular to the direction of flow via

$$\dot{m} = J_{KK}S, \tag{11}$$

where S is the internal cross-sectional area of the tube or vessel containing the flow and the dot over the variable explicitly indicates the time derivative. Thus, the dependence of flux on vessel diameter is clearly indicated.

2.2 Relationship of the Diffusion with Drift Equation to Contrast: Random Motion and the Lorentzian Cumulative Distribution Function

Consider the 1-D case[9]

$$J_{KK} = -D\frac{\partial[c]}{\partial x} + \vec{v}_x[c]. \tag{12}$$

From the above equation, it is seen that the total flux, J_{KK}, is dependent upon the concentration (gradient) of scatterers, $[c]$, and the velocity, $\vec{v}$, of the surrounding fluid that is causing a lateral translation of the scatterers. Note that changes in $[c]$ manifest as changes in the scattering coefficient, μ_s, of the fluid solution under observation.

The first term on the RHS of Eq. (12) is recognized as Fick's first law of diffusion.[9] Particle motion described by this term is random (Brownian). Fercher and Briers[1] invoked this assumption about the particle motion in their initial description LSCI. Under this assumption, a relationship between speckle contrast, K, (in the imaging plane) and the exponential (de)correlation function associated with Brownian motion has been developed by several authors[2,3] and serves as one possible limiting behavior[8]

$$K(\bar{r}) = \left\{\frac{\tau_c}{2T}\left[2 - \frac{\tau_c}{T}\left(1 - e^{-2T/\tau_c}\right)\right]\right\}^{\frac{1}{2}}, \tag{13}$$

where τ_c is the characteristic decorrelation time of the observed speckle pattern in the imaging plane and T is the camera integration time. It is important to note that Eq. (13) is actually the cumulative distribution function of a Lorentzian probability distribution function.[8]

2.3 Ordered Flow and the Gaussian Cumulative Distribution Function

Equation (13) is technically only correct for purely random particle motion described by the first term on the RHS of Eq. (13). This term, $-D(\partial[c]/\partial x)$, describes the diffusional flux, J_L, component of J_{KK}. In this motion, the individual behaviors of the particles are representative of the population as a whole.

The second term on the RHS of Eq. (13) describes the advective flux, J_G, component of J_{KK}. This term, $\vec{v}[c]$, describes ordered motion of the particles and the dynamic behavior of the individual particles is unique to the individual scatterers. That is, the behavior of individual particles is not representative of the behavior of the population. This behavior forms the other possible limiting behavior of dynamic particles. As above, several authors have presented a relationship between the observed speckle contrast and the Gaussian correlation function associated with ordered motion[2,3]

$$K(\bar{r}) = \left\{ \frac{\tau_c}{2T} \left[\sqrt{2\pi} \mathrm{erf}\left(\frac{\sqrt{2}T}{\tau_c} \right) - \frac{\tau_c}{T} \left(1 - e^{-2(T/\tau_c)^2} \right) \right] \right\}^{\frac{1}{2}}.$$
(14)

Again, it is worth noting that the above equation is in actuality a cumulative distribution function of a Gaussian probability distribution function. Also worth noting is that Eq. (14) is technically only accurate for purely ordered flow.[8]

2.4 Combination of Ordered and Unordered Flow

It is becoming clear that LSCI is sensitive to flux, J. The previous two sections have discussed the two contributions to J_{KK}, diffusional flux, J_L, and advective flux, J_G. In most practical situations involving LSCI, it is most likely that both forms of motion are present in some proportion and the actual behavior is a mixture of these two statistically independent processes. In this case, the model relating K to the characteristic correlation behavior of the scatterers would be a convolution of the two previous models. Note that by the convolution theorem,[8] the net correlation function for the combined behavior is simply the product of the exponential correlation behavior associated with random motion and the Gaussian correlation behavior associated with ordered motion. Such a model is referred to as a Voigt model.[8] This model has been discussed by Duncan and Kirkpatrick[8] and has been shown to have physical relevance with regards to relating speckle correlation times to scatterer velocity in the object plane. A clear association between flux and decorrelation time has yet to be presented in the literature and is beyond the scope of this paper. This is a topic for further development.

Thus, depending upon the implementation of LSCI, LSCI is sensitive to diffusional flux [Eq. (9)], advective flux [Eq. (10)], or some combination of the two [Eq. (12)]. In most practical scenarios of interest, LSCI depends upon both velocity and concentration.

3 Materials and Methods

A small flow system, an LSCI system, and a series of fluid phantoms with known optical properties were developed so as to examine the effects of velocity, $\vec{v}$, and scatterer concentration, $[c]$. Because the direction of the flow was known *a priori*, velocity, not speed was evaluated. A polarized 660-nm diode laser

(B&W Tek, Newark, Delaware) illuminated a piece of glass tubing with an outer diameter of 2 mm and an inner diameter of 1.5 mm on top of a grooved plastic base. The size of the tube is somewhat large in comparison to the smaller vessels usually imaged with LSCI. However, this does not change the results of this paper. The illuminated region was ~20 mm in length. The glass tube, which served as our imaging window, rested in the groove. Thus, there was a layer of static scatterers below the flow tube and along both sides. The static scattering regions adjacent to the flow tube served as reference regions to normalize the contrast values from the flow region (see below). A section of rubber tubing was attached to the glass tubing that connected the tubing system to a mini peristaltic pump (Instech Laboratories, Plymouth Meeting, Pennsylvania, model P625). The fluid phantom material flowed into the tubing using this mini peristaltic pump, which was controlled by an Arduino microcontroller. A MATLAB® graphical user interface (GUI) controlled the CCD camera (Point Grey, Dragonfly, Vancouver, BC, Canada) and the pump, and also calculated and saved contrast images in near real-time (Fig. 1).

Scattering flow phantoms were made by mixing aluminum borosilicate glass microspheres (Luxil Cosmetic Microspheres, Potters Industries, Inc., Malvern, Pennsylvania) with deionized water (DI) water. The microspheres were polydispersed in terms of size and the diameters nominally ranged between 9 and 13 μm with a mean diameter of 11.7 μm according to the manufacturer. The sphere diameters were slightly larger than typical red blood cells, which have a diameter in the range of 6 and 8 μm. This difference in scattering properties, however, between the spheres we employed and spheres with diameters in the 6- to 8-μm range is relatively insignificant at the wavelength we used. The number distribution of the sizes was not known to us. The microspheres had a mass density of 1.1 g/cc. Using Mie theory, we calculated the appropriate concentrations to create scattering solutions with reduced scattering coefficients, μ_s', that approximated that of whole blood with various hematocrit levels.[10] Once the solutions were mixed, ballistic transmission measurements were used to verify the scattering coefficient, μ_s and ultimately, μ_s'. The concentration of microspheres used was lower than the normal concentration of blood cells, however, the scattering properties of our phantom fluids and that of whole blood at different hematocrit levels were similar.

A modified version of the Lambert–Beer law was used to calculate the scattering coefficient from the ballistic transmission data. Since only scatterers were added to the DI water,
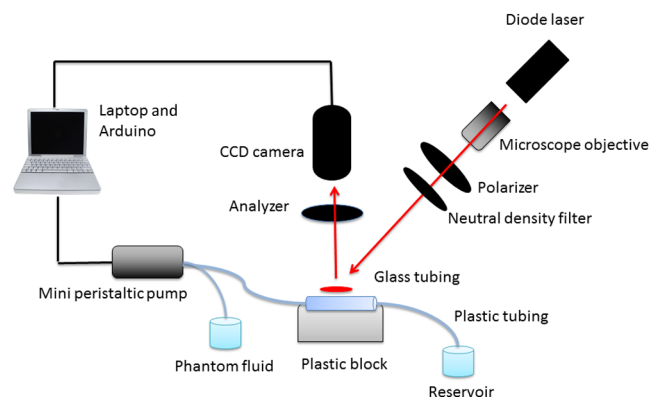

Fig. 1 Diagram of the LSCI and flow systems.

we assumed that the scattering coefficient was much greater than the absorption coefficient, μ_a, and that $\mu_a = 0$. Thus

$$I(z) = I_0[\exp{-(\mu_s + \mu_a)z}]; \quad \mu_a = 0, \quad (15)$$

$$\mu_s = \frac{\ln\left[\frac{I(z)}{I_0}\right]}{z}, \quad (16)$$

where z is the thickness of the samples (1.0 cm) and I_0 was the measured intensity of the ballistically transmitted beam when pure DI water was used as the sample. Since the ballistic intensity of the DI water and the scattering samples was measured in the same cuvette and the ratio between the intensities, $I(z)/I_0$, the intensity loss due to the cuvette wall was eliminated from the calculations.

Assuming scattering anisotropy $g = 0.9$ based on the Mie calculations, μ_s' was calculated for the phantoms as

$$\mu_s' = \mu_s(1 - g). \quad (17)$$

In this fashion, 10 liquid phantom samples were made. The number concentration, $[c]$, of microspheres ranged from 1×10^{-5} to 1×10^{-4} microspheres/μm^3 and the reduced scattering coefficients of the samples ranged from 0.48 to 4.84 mm^{-1}. Pure DI water was also used as a flow sample.

Each fluid phantom was run through the LSCI system described above. Figure 2 shows the cross-section of the sample preparation we used in the LSCI setup. As can be seen in the figure, both moving and static scatterers were within the DOF of the imaging lens and thus the light scattering from these different regions summed coherently into a single speckle pattern. In this figure, the flow is coming out of the page, toward the reader. The laser was set slightly off-axis to avoid specular reflection. A video of 100 frames was recorded with a CCD camera for each sample at 125 frames/s. The custom MATLAB® GUI saved all 100 frames of the raw speckle patterns, generated contrast images using a sliding 7×7 pixel window,[11] and finally saved the resulting contrast images. The experiment was repeated three times for each sample. In order to more generalize the results, we reported a value of $K_{ratio} = K_{flow}/K_{static}$, where K_{flow} is the contrast calculated from the 7×7 pixel window cropped from the flow region of the speckle images and K_{static} is an identically sized window from the surrounding static
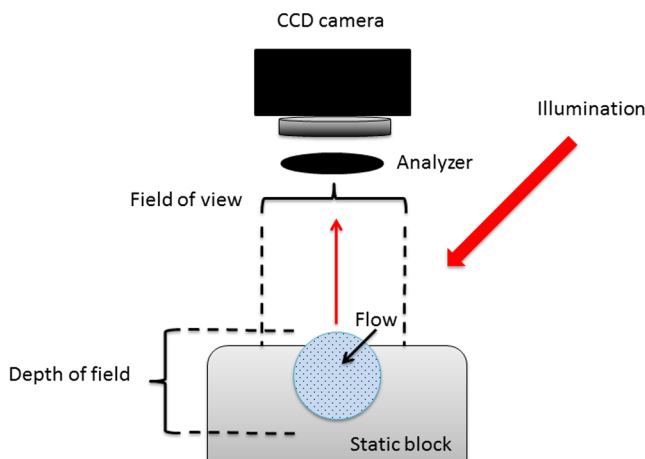
region. Reporting K_{ratio} as opposed to just reporting values of K reduced the undesirable influences of ambient light and fluctuations in incident laser intensity on the sample, as well as reducing the influence of the scattering properties of the background static block on the results.

During the experiments to examine the sensitivity of LSCI to changes in $[c]$, all of the experimental variables were held constant with the exception of μ_s', which varied by sample. The velocity, $\vec{v} = 5.0$ mm/s, the outer diameter of the glass tubing was 3 mm and the inner diameter was 2 mm. The camera integration time, T, was 6 ms. The camera lens (55-mm telecentric lens) was fixed at $f/32$, which resulted in relatively large speckles and an extended DOF. The minimum speckle size on the CCD chip in the camera was $\sim 3\times$ the pixel pitch as determined by examining the power spectrum of a speckle image. K_{ratio} values were calculated as above and plotted as a function of particle concentration.

Similarly, to examine the changes in $\vec{v}$, fluid phantoms with a single $[c]$ were flowed through our fluids system at varying velocities ranging from 1 to 8 mm s^{-1}. The particle concentration of these samples was constant at 6×10^{-5} spheres/μm^3, which resulted in a reduced scattering coefficient of 2.2 mm^{-1}. All other experimental variables were held constant at the same values as above. K_{ratio} values were calculated and plotted as a function of velocity.

Thus our experiments individually assessed the sensitivity to both $[c]$ and $\vec{v}$, i.e., to both components of advective flux.

4 Results

The experiments described above were designed specifically to assess the sensitivity to the $\vec{v}[c]$ term of Eq. (12) and the results clearly show a dependence of K_{ratio} on this term, i.e., on advective flux, $\vec{v}[c]$. Both individual changes in $\vec{v}$ and $[c]$ result in changes in K_{ratio}. Figures 3(a) and 3(b) show the results of the experiments aimed at assessing the sensitivity of LSCI to scattering particle concentration, $[c]$. Figure 3(a) shows the results in terms of changes in μ_s', while Fig. 3(b) shows the results directly in terms of particle concentration. The velocity of the fluid in these experiments was 5.0 mm s^{-1}. The solid lines represent the best-fit line in a least-squares sense. The linear equations for these lines are, respectively,

$$K_{ratio} = -0.072\mu_s' + 0.0965,$$
$$K_{ratio} = -3.3 \times 10^{-3}[c] + 0.982. \quad (18)$$

Correlation coefficients for the relationships were $r^2 = 0.95$ and $r^2 = 0.97$, respectively. Thus there is a strong, linear negative relationship between the concentration of scatterers and speckle contrast. Of note in both plots are the points where $[c] = 0$, i.e., when contrast measurements were made using pure DI water. The K_{ratio} values in these cases were 0.9985, 0.9986, and 0.9984. These values indicate that the glass tubing used in our experimental flow system had negligible influence on the contrast values. That is, the contrast in the glass tube was the same as the contrast in the surrounding static medium when no dynamic scatterers were present. Thus, no correction for background scatter from the tube was necessary.

The next set of experiments examined the relationship between the velocity of the moving fluid and speckle contrast. Recall from above, that these experiments were conducted with samples having a $\mu_s' = 2.2$ mm^{-1}. This value was somewhat arbitrarily chosen because it lies near the middle of the range
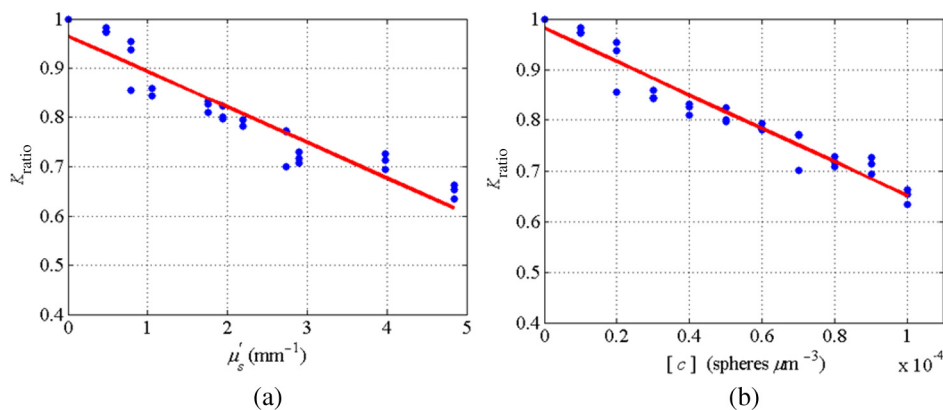

CCD camera

Illumination

Analyzer

Field of view

Flow

Depth of field

Static block

Fig. 2 Sample cross-section.

(a)   (b)

Fig. 3 (a) K_{ratio} versus reduced scattering coefficient. A strong negative correlation ($r^2 = 0.95$) was found between the two variables. The slope of the best-fit line was -0.072. (b) K_{ratio} versus scatterer concentration. A strong negative correlation ($r^2 = 0.97$) was found between the two variables. The slope of the best-fit line was -3.3×10^{-3}.
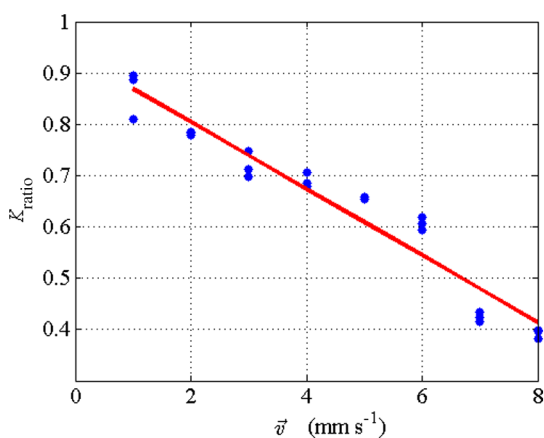

Fig. 4 Relationship between speckle contrast and the velocity of the moving fluid. The fluid phantom had a reduced scattering coefficient of 2.2 mms^{-1}. The correlation coefficient, $r^2 = 0.96$.

of the scattering coefficients we examined. As above, a strong negative linear correlation was found between K_{ratio} and $\vec{v}$. The results are shown in Fig. (4). The linear least-squares regression line was described by the following equation

$$K_{\text{ratio}} = -0.065\vec{v} + 0.934 \quad (r^2 = 0.96). \tag{19}$$

It is worth noting that the slope of this line is of the same order as the slope of the K_{ratio} versus μ_s' line. This observation appears to indicate that LSCI is equally sensitive to changes in velocity and scatterer concentration.

Combining the above results allows for an investigation into the sensitivity of LSCI to advective flux, $\vec{v}[c]$. Because the results thus far indicate equal sensitivity to both velocity and scatterer concentration, $\vec{v}$ was held constant at $\vec{v} = 5$ mms^{-1} and $[c]$ was varied from $0 \leq [c] \leq 1 \times 10^{-4}$ spheres/μm^3. Figure 5 shows the dependency of K_{ratio} on $\vec{v}[c]$.

Speckle contrast was found to decrease monotonically with increasing advective flux following the linear relationship

$$K_{\text{ratio}} = -0.66\vec{v}[c] + 0.982 \quad (r^2 = 0.97). \tag{20}$$

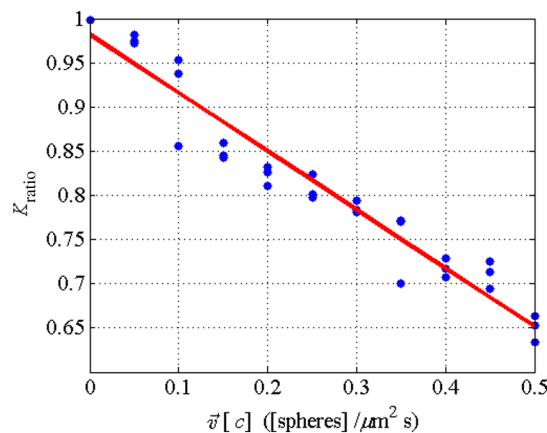This result clearly demonstrates that LSCI is sensitive to advective flux.

Fig. 5 Relationship between K_{ratio} and advective flux. A strong negative linear relationship was found ($r^2 = 0.97$).

It is certainly worth noting that the y-intercept is $\sim$1.0. It was demonstrated above that the glass tube had essentially no influence on the contrast values, so a y-intercept of 1.0 should be expected, assuming, as we did, that the first term on the RHS of Eq. (12), that is the diffusive flux term, $(\partial[c]/\partial x) = 0$. That the y-intercept is $\sim$1.0, then, confirms the assertion that these experiments explicitly examined the influence of advective flux on LSCI.

5 Discussion

The results clearly demonstrate a negative linear dependence of K on both $[c]$ and $\vec{v}$ for our experimental arrangement. It is worth noting that the experimental results presented herein indicate that LSCI is approximately equally sensitive to both changes in velocity and changes in scatterer concentration. This is significant in that a change in scatterer concentration may be mistaken for a change in velocity when using LSCI. This implies that to properly interpret LSCI data, which is typically used to assess a change in blood flow (or speed, or velocity), a change in scatterer concentration must be either logically or experimentally ruled out. Such a change may arise from a change in hematocrit level. In most studies, a change in hematocrit can be ruled out physiologically. However, one could envision LSCI being used in time-course studies where a change in

hematocrit is possible or when comparing LSCI results between individuals, who may have different hematocrit. In these cases, the results presented here indicate that $[c]$ must be considered in the interpretation of those results. A more detailed analysis of this is needed.

It should be noted that our results indicate a negative linear relationship between speckle contrast and velocity (the term velocity is known because we know the full vector *a priori*). Other researchers have reported a negative exponential relationship between speckle contrast and velocity when employing temporal speckle contrast imaging.[12] It is obvious that contrast values will approach zero at some velocity that is dependent upon the flow and imaging geometries. Through the range of velocities explored herein, however, contrast remained linearly related to velocity. Had higher, very nonphysiological velocities been explored, it is likely that this relationship would have become nonlinear and asymptotically approached zero, perhaps following a negative exponential relationship described by Li et al.[12] It is worth noting that other authors have suggested a linear relationship between contrast and velocity when using spatial speckle contrast imaging.[13,14] It is expected that speckle contrast imaging will exhibit the same dependence on advective flux, regardless of whether the speckle data are processed in the spatial or temporal sense.

Our experiments were intentionally devised so as to focus on the second term on the RHS of Eq. (12), i.e., our experimental arrangement focused on the sensitivity of LSCI to advective flux, $\vec{v}[c]$. An underlying assumption is that the diffusional flux term of Eq. (12) is small, i.e., $-D\frac{\partial[c]}{\partial x} \ll \vec{v}_x[c]$. Other studies have focused more on the diffusional flux term, and although not couched in mass-transport terms, demonstrated a clear dependence of LSCI on $\partial[c]/\partial x$.[15]

It is worth asking the question of how to interpret the *y*-intercept of Fig. (5) had it not been unity and was something >1.0. The theoretical development and the experimental results appear to indicate that any reduction in K_{ratio} when $\vec{v}[c] = 0$ must be due to random diffusional flux [i.e., the first term on the RHS of Eq. (12)] in the absence of absorption. Thus, the theory and experiments in this paper suggest an approach to determining the relative contributions of diffusional flux (unordered motion) and advective flux (ordered motion) to the reduction in speckle contrast, if absorption is negligibly small or otherwise known. This is discussed in more detail below with regards to choosing a proper statistical model to relate speckle contrast to particle motion.

Another issue to consider is that in our experiments, a solid, static scattering block was below and in the same DOF as the dynamic, flowing scatterers. One could argue that our experiments merely demonstrate that as $[c]$ increases, the influence of the static scatterers, which by themselves should result in a high contrast value of $K \to 1.0$ is reduced. The usual argument explaining this phenomenon is that as more and more moving scatterers are introduced to the imaged volume, the number of speckle fluctuations will also be increased, diminishing the overall influence of the static scatterers. If we were considering LDF, we would make the argument that the fraction of Doppler-shifted photons increases with an increase in the number of scatterers.[3] Indeed, these arguments are correct. However, they do not diminish our results that indicate that LSCI is sensitive to advective flux.

The one cautionary note regarding the influence of static scatterers is that the proportionality constants that we report relating K_{ratio} to $[c]$ may not be entirely generalizable and may vary depending upon the experimental arrangement due to the scattering properties of the background material. However, by reporting K_{ratio} values as opposed to purely values of K, this influence of background scatterers is reduced and the results should be fairly generalizable. Note that in living tissue, there are no scattering volumes in which the speckle arising from the volumes has a decorrelation time $\tau_c \to \infty$. That is, there are no static scatterers and speckle from living tissue will always have a finite τ_c. Thus, reporting values of K_{ratio} might not always be possible in actual applications of LSCI, however, it should be noted that $K_{ratio} \propto K$.

Another consideration is that as red blood cells move through vessels, they tumble. This tumbling motion may lead to additional speckle fluctuations that may reduce the contrast values. This is a limitation to our flow phantom studies and an area that requires further investigation. However, it does not alter our primary conclusion that LSCI is sensitive to advective flux.

The question of the proper statistical model for describing the underlying motion of the scattering particles and ultimately relating this model to the observed contrast arises frequently in the LSCI literature where it is either directly addressed,[2,3] or one statistical model or the other is implicit in the analysis.[5] The two limiting behaviors as discussed above in Sec. 2 are random (Brownian) motion and ordered motion. Ultimately, these two limiting behaviors give rise to Lorentzian and Gaussian correlation functions, respectively, that relate contrast K and the decorrelation time, τ_c, of the observed speckle. Frequently, the discussion surrounding the proper choice of the statistical model gives the appearance that this is a binary choice. One has to either assume a Gaussian or a Lorentzian model. Although it has been proposed that a Voigt model might be a logical alternative and that this Voigt model is a convolution of the Lorentzian and Gaussian line shapes.[8]

The theoretical development, above, resulting in Eq. (7) for the two-dimensional case and Eq. (12) for the 1-D case, along with the experimental findings, lends credence to the choice of a Voigt model. From these equations, it becomes apparent that this model selection is not binary, but is actually points along a continuum, with the Lorentzian and Gaussian models serving only as the outer limits to the continuum. Inspection of Eq. (12) reveals that LSCI is sensitive to both diffusive flux, J_L and advective flux, J_G, where the total flux, $J_{KK} = J_L + J_G$. If the particle motion is assumed to be entirely random (Brownian), then LSCI is revealing J_L and the Lorentzian model should be adopted. Alternatively, if the particle motion is assumed to be entirely ordered, then LSCI is revealing J_G and the Gaussian model should be adopted. However, in most normal cases of interest both components of total flux will be present and the appropriate statistical model is some combination between the Lorentzian and Gaussian models. As suggested above, one solution to this is to employ a Voigt model,[8] which is the convolution of the Lorentzian and Gaussian models, or some other weighted linear combination of the two, where the weights reflect the relative contributions of diffusive flux and advective flux. Readers are referred to Duncan and Kirkpatrick[8] for more details on this model. When viewed in terms of mass transport, then, it becomes apparent that the oft cited binary decision between the Lorentzian and Gaussian models is a false decision and that these two models are simply limiting behaviors governed by the diffusion with

drift equation.[9] As noted in Sec. 2, a clear relationship between flux, flow model, speckle contrast, and decorrelation time of the speckle has not yet been fully developed and presented in the literature. Some authors, notably Kazmi et al.[13] have made some progress in this area, however.

In summary, we have viewed LSCI from a mass-transport perspective and demonstrated that by adopting the diffusion with drift equation [Eq. (12) for the 1-D case], a theoretical basis for understanding the sensitivity of LSCI to both particle concentration and speed (or velocity) can be shown. Furthermore, this same mass-transport approach, invoking the diffusion with drift equation, draws a mathematical and physical linkage between random and ordered motion of particles. This single equation [e.g., Eq. (12)] adequately describes both behaviors as limiting conditions on contrast values. Finally, when discussing LSCI, we encourage the use of the term flux and, in particular, diffusive flux and advective flux (as opposed to terms such as perfusion, flow, velocity, and speed) to describe the physical variable to which LSCI is sensitive.

References

1. A. F. Fercher and J. D. Briers, "Flow visualization by means of single-exposure speckle photography," *Opt. Commun.* **37**(5), 326–330 (1981).
2. D. A. Boas and A. K. Dunn, "Laser speckle contrast imaging in biomedicine," *J. Biomed. Opt.* **15**(1), 011109 (2010).
3. D. Briers et al., "Laser speckle contrast imaging: theoretical and practical limitations," *J. Biomed. Opt.* **18**(6), 066018 (2013).
4. R. Bonner and R. Nossal, "Model for laser Doppler measurements of blood flow in tissue," *Appl. Opt.* **20**(12), 2097–2107 (1981).
5. A. Dunn et al., "Dynamic imaging of cerebral blood flow using laser speckle," *J. Cereb. Blood Flow Metab.* **21**, 195–201 (2001).
6. B. J. Kirby, *Micro- and Nanoscale Fluid Mechanics*, Cambridge University Press, Cambridge, United Kingdom (2010).
7. J. W. Goodman, "Some effects of target-induced scintillationson optical radar performance," *Proc. IEEE* **53**(11), 1688–1700 (1965).
8. D. D. Duncan and S. J. Kirkpatrick, "Can laser speckle flowmetry be made a quantitative tool?" *J. Opt. Soc. Am. A* **25**(8), 2088–2094 (2008).
9. H. C. Berg, *Random Walks in Biology*, Princeton University Press, Princeton, New Jersey (1983).
10. M. Hammer, A. N. Yaroslavsky, and D. Schweitzer, "A scattering phase function for blood with physiological haematocrit," *Phys. Med. Biol.* **46**, N65–N69 (2001).
11. D. D. Duncan, S. J. Kirkpatrick, and R. K. Wang, "Statistics of local speckle contrast," *J. Opt. Soc. Am. A* **25**, 9–15 (2008).
12. P. Li et al., "Imaging cerebral blood flow through the intact rat skull with temporal laser speckle imaging," *Opt. Lett.* **31**(12), 1824–1826 (2006).
13. S. M. Kazmi et al., "Flux or speed? Examining speckle contrast imaging of vascular flows," *Biomed. Opt. Express* **6**(7), 2588–2608 (2015).
14. A. K. Dunn et al., "Dynamic imaging of cerebral blood flow using laser speckle," *J. Cereb. Blood Flow Metab.* **21**, 195–201 (2001).
15. R. Bandyopadhyay et al., "Speckle-visibility spectroscopy: a tool to study time-varying dynamics," *Rev. Sci. Instrum.* **76**, 093110 (2005).

Biographies for the authors are not available.